JOURNAL OF CATALYSIS **173,** 345–354 (1998)
ARTICLE NO. CA971926

Influences of Some Synthesis Parameters and Activation Procedures on the One-Step Sol–Gel Synthesis of Sulfated-Zirconia Catalysts, Followed by TG-DSC and Mass Spectrometry

H. Armendariz, B. Coq,[1] D. Tichit, R. Dutartre, and F. Figuéras[2]

Laboratoire de Matériaux Catalytiques et Catalyse en Chimie Organique, UMR 5618 du CNRS, 8 rue de l'Ecole Normale, 34296 Montpellier Cedex 1, France

Received May 19, 1997; revised September 8, 1997; accepted September 8, 1997

A series of sulfated zirconia (SZ) were prepared by sol–gel methods, from Zr *n*-propoxide, either with the *in situ* one-step addition of H_2SO_4 during the gelification process, or by *ex situ* sulfation of a $Zr(OH)_4$ hydroxide. Several parameters were studied for the *in situ* sol–gel preparation: (i) the H_2O/Zr^{IV} hydrolysis ratio, (ii) the protocol followed for the sulfate introduction, and (iii) the amount of sulfate (6 to 30%) added. The activation of SZ was followed by TG-DSC and mass spectrometry detection. The textural properties of SZ are dependent on both the hydrolysis ratio and the procedure for H_2SO_4 introduction. SZ prepared when introducing H_2SO_4 through hydrolysis water exhibited a narrow distribution of mesopores centered around 2–3 nm and intergranular macroporosity which increased with the hydrolysis ratio. SZ prepared by introducing H_2SO_4 through Zr *n*-propoxide solution exhibited a wide distribution of large mesopores from 3 to 20 nm. In all cases the introduction of sulfate delayed the crystallization into the tetragonal phase. The endothermic decomposition of sulfate species occurs at the beginning of the tetragonal to monoclinic transition. Their catalytic properties were evaluated in the hydroconversion of *n*-hexane using mechanical mixtures of SZ and Pt/Al_2O_3. SZ's prepared by *in situ* methods are the most active catalysts. The rate became maximum for a S content close to a nominal monolayer of sulfate after activation at ca 900 K in air. The SZ thus prepared, by *in situ* methods, were twentyfold more active, per nominal sulfate site, than SZ prepared by *ex situ* sulfation. This higher reactivity was attributed to acid sites of the same type as previously proposed by Kustov *et al.* (*J. Catal.* 150, 143 (1994)).

Key Words: **sulfated zirconia; sol–gel; *n*-hexane hydroconversion; thermal analysis.**

1. INTRODUCTION

There is a great need to develop new solid acid catalysts that are active and stable at low temperatures for the synthesis of reformulated gasolines. Zirconia doped with some anions, sulfate in particular, belongs to this category. The doping effect of sulfur on specific surface areas, crystallographic phase transitions, and sintering of the zirconia is now well established. The stability and the surface acidity of sulfated-zirconia (denoted in the text as SZ) are indeed directly dependent on the textural properties of the parent zirconium hydroxide and on the sulfation process (1). Even if super-acid properties have initially been claimed (2), this point remains still controversial, in particular under a hydrogen atmosphere (3).

The classical preparation of SZ proceeds by precipitation of an aqueous zirconium salt solution with a base; the zirconium hydroxide ($Zr(OH)_4$) thus obtained is then sulfated by immersion in sulfuric acid or by impregnation with ammonium sulfate (1). An alternative preparation proceeds through a sol–gel method, allowing the one-step synthesis of SZ aerogels (4–6) or xerogels (6, 7). When compared to SZ prepared by the classical methods, these materials prepared by one-step sol–gel synthesis, containing similar S content and calcined at the same temperature, exhibit larger surface areas, controlled porosity, and higher reactivity for hydrocarbon conversions under N_2 or H_2 atmospheres (5–7). The one-step sol–gel synthesis of SZ consists in the addition of water to an alcohol solution of zirconium alkoxide, the sulfuric acid being introduced either through the alkoxide solution (4–7), or through the hydrolysis water (7). After gelification and condensation of the precursor, a supercritical drying leads to aerogels (4–6), xerogels being obtained by drying between 350 and 400 K under atmospheric pressure (7). Further calcination steps at temperatures higher than 823 K led to catalytically active SZ catalysts.

This sol–gel method thus appears very useful to prepare highly active SZ catalysts in a one-step process. However, the structure of the condensed gels depends on several parameters (8). It was thus one of the objectives of this work to study the influence of some of the preparation parameters: (i) the H_2O/Zr^{4+} molar ratio; (ii) the introduction of sulfate, either through hydrolysis water or through alkoxide solution; and (iii) the sulfate content, on the properties of SZ's

[1] To whom correspondence should be addressed. E-mail: coq@cit.enscm.fr.

[2] Present address: Institut de Recherche sur la Catalyse du CNRS, 2 Av. A. Einstein, 69626 Villeurbanne, France.

0021-9517/98 $25.00

prepared by a one-step procedure. Special emphasis was addressed to the nature of the phenomena occurring during the activation procedures: phase transitions, evolved gases, and decomposed species, which were followed by TG-DSC and mass spectrometry.

The catalytic properties of the synthesized SZ's were evaluated in the hydroconversion of *n*-hexane (nH) at atmospheric pressure. Until now the debate remains open about the exact nature of the mechanism operating during the hydroconversion of alkanes on SZ promoted with a metallic function (6, 9–15). The problem is actually the state of the metallic function. Ebitani *et al.* (9) concluded that, after calcination at 873 K and reduction at 523 K, Pt is mainly in the oxidized state in Pt/SZ. In contrast, Pt was claimed already reduced after calcination at 873 K, and further treatment in H_2 did not change the state of the Pt, which is hardly accessible to H_2 chemisorption due to poisoning by sulfur adspecies (6b, 13, 16–18). However, when Pt/SZ was calcined at 773 K and reduced at 523 K, Pt was reduced and exhibited good accessibility to H_2 (19). Unfortunately, high temperatures of calcination ($\geq$873 K) are needed to develop the strong acidity of SZ. On the other hand, ideal bifunctional acid catalysts can be obtained by the use of mechanical mixtures of an oxide-supported metal catalyst with the solid acid (20). Yori *et al.* (13) have thus shown that, in a mechanical mixture of Pt/Al_2O_3 and SZ, precalcined at 890 K, Pt is very likely reduced, and accessible, after a direct treatment in H_2 at 573 K. Thereby, the hydroconversion of *n*-butane, on this catalyst, operated through a bifunctional mechanism. In this work, we have thus studied the nH hydroconversion on mechanical mixtures of SZ and Pt/Al_2O_3.

2. EXPERIMENTAL

2.1. Catalysts Preparation

The alkoxide precursor for the sol–gel preparations was zirconium *n*-propoxide ($Zr(OC_3H_7)_4$, 70 wt% in *n*-propanol, Aldrich) and the solvent was *n*-propanol (99% purity, EDS). Sulfate source was provided by sulfuric acid (94–96%, EDS).

In the general procedure, 20 cm^3 of zirconium *n*-propoxide was mixed with 26.6 cm^3 of *n*-propanol in one beaker and stirred with a magnetic stir bar. Different amounts of water (from 0.8 to 3.7 cm^3) were then added dropwise in order to carry out the hydrolysis and gelation of zirconium alkoxide. The addition of hydrolysis water takes about 5 min. When formed, the gel was aged for 1 h at room temperature; it was then placed into an oil bath at 348 K to remove alcohol. The solid was then dried at 393 K for 12 h. Finally, the solids were calcined at different temperatures up to 923 K for 4 h in flowing air (4 $dm^3\ h^{-1}$) in a quartz tube inside a tubular furnace.

When the hydrolysis was performed in acid medium, the presence of sulfuric acid led in one step to a sulfated alcogel which, after drying and calcination, gave the SZ sample, *in situ* sulfation. Following this procedure two methods can be considered. On the one hand, sulfuric acid was introduced in the solution of zirconium alkoxide in *n*-propanol; water was then added dropwise to complete hydrolysis (method *isA*). This method was previously used to prepare SZ's (4, 5) and Pt/SZ (6). On the other hand, an aqueous solution of sulfuric acid was added dropwise into the mixture of zirconium alkoxide and *n*-propanol (method *isB*). For one sample, the hydrolysis was performed in a neutral medium by the addition of water alone; a zirconia xerogel was thus obtained. After drying it was sulfated by impregnation with sulfuric acid, *ex situ* sulfation (method *esC*).

The Pt/Al_2O_3 used for mechanical mixtures with SZ was prepared by ion exchange between H_2PtCl_6 and γ-Al_2O_3 ($S_{BET} \approx 200\ m^2\ g^{-1}$). The final catalyst contains 0.37 wt% Pt, with H/Pt $\approx$ 0.9; it does not exhibit any activity for *n*-hexane hydroconversion at 423 K.

2.2. Characterization of the Catalysts

The zirconia samples and their activation were characterized by chemical analysis, X-ray diffraction, N_2 physisorption, differential scanning calorimetry (DSC) with thermogravimetry (TG) attachment, and mass spectrometry (MS). Chemical analyses of the samples were performed at the Service Central d'Analyse du CNRS (Vernaison, France). X-ray diffraction patterns were recorded on a CGR theta 60 instrument with the Cu Kα1 radiation. Nitrogen isotherms at 77 K were obtained by using a Micromeritics ASAP 2000 apparatus; the samples were previously outgassed under vacuum at 523 K overnight.

TG-DSC experiments were carried out in a SETARAM TG-DSC-111 apparatus, with fully programmable heating and cooling sequences, sweep gas valve switchings, and data analysis. About 50 mg of sample were placed in a platinum crucible and dried at 393 K under He stream (flow: 20 $cm^3\ min^{-1}$). Heating was then started at 10 K min^{-1} from room temperature up to 1173 K in a stream of synthetic air (flow: 20 $cm^3\ min^{-1}$).

A Balzers QMS 421 quadrupole mass spectrometer equipped with a SEM detector (0–200 amu) was used to conduct analysis of the evolved gases during parallel experiments such as TG-DSC, under exactly the same conditions of activation, nature of the gases, and temperature ramp. The sample bed ($\approx$100 mg) was placed in a quartz reactor. The composition of the gases flowing from the reactor was monitored continuously on-line by sampling through a fused silica capillary transfer line (flow in the capillary $\approx$20 $cm^3\ min^{-1}$). Self-resistant heating was done to prevent condensation inside the capillary. Up to 64 masses can be concurrently monitored. The masses selected during our experiments corresponded to those of sulfur compounds (34, 48, 64, 80), *n*-propanol (31), 1-propene (41, 42), CO_2 (44), and H_2O (18).

2.3. *n*-Hexane Hydroconversion

The reaction of *n*-hexane (nH, Carlo Erba > 99%) with hydrogen (AGA, high purity grade > 99.99%) was carried out at atmospheric pressure in a dynamic glass reactor. The partial pressure of nH was maintained at 6.04 kPa ($P(H_2)/P(nH) = 17$, $WHSV(nH) = 0.81\ h^{-1}$). The effluents were analysed by sampling on-line to a FID gas chromatograph equipped with a J & W capillary column (60 m × 0.5 mm ID DB1 apolar bonded phase). After calcination of SZ at the dedicated temperature for 4 h, a mechanical mixture of SZ (≈100 mg) and $Pt/\gamma\text{-}Al_2O_3$ (usually 300 mg) was prepared, charged in the reactor, and reduced under H_2 flow at 623 K for 2 h (flow: 20 $cm^3\ min^{-1}$, ramp 2 K min^{-1}). After cooling, the reaction was started at 423 K. The following parameters were evaluated:

$$\text{conversion (mol\%)} = \left(\sum_1^6 (i/6)C_i\right) \Big/ \left(C_6^0 + \sum_1^6 (i/6)C_i\right) \times 100$$

selectivity S_i to compound i:

$$S_i\ (\text{mol\%}) = C_i \Big/ \left(\sum_1^6 C_i\right) \times 100,$$

where C_i is the mole percent in the feed of product with i carbon atoms and C_6^0 is the mole percent in the feed of nH.

3. RESULTS

3.1. Behavior of a Mechanical Mixture of SZ and Pt/Al_2O_3

It should be noted that Pt/Al_2O_3 did not exhibit any activity for nH conversion in the temperature range investigated. As discussed in the Introduction, the state of Pt and the extent of free surface of Pt^0 after H_2 activation are open to discussion. In the mechanical mixture of SZ and Pt/Al_2O_3, the Pt surface will depend on the amount of Pt/Al_2O_3, as well as on the temperature of reduction. In Fig. 1 the nH conversion at 423 K is plotted as a function of these two factors for the SZ(4)*isB*(3.2) sample which was the most active SZ after calcination at 898 K. One can see that the nH conversion goes through a maximum for $(Pt/Al_2O_3)/SZ(4)isB(3.2) \geq 3$ (wt/wt). The conversion was recorded after 10 min under stream; the activity tended to stabilize after 3 h, where the conversion was diminished by a factor 2–3. On the other hand, the larger extent of active Pt^0 surface is probably obtained after reduction of the mechanical mixture at 620 K. This is a compromise between the reduction of "PtO" species, which increases steadily with the temperature and the poisoning of the reduced Pt^0 surface by sulfur species. Moreover, a too-high temperature leads to Pt sintering. A TPR experiment, indeed, showed that reduction of sulfate species, by H_2, had already begun at 570 K in the presence of Pt (6b, 9, 19, 21). Under these conditions, after reduction at 620 K of a $SZ + Pt/Al_2O_3$ mixture (1/3, wt/wt), the metallic Pt surface should be large enough to obtain dehydrogenating/hydrogenating properties and to promote the occurrence of a bifunctional mechanism (13).

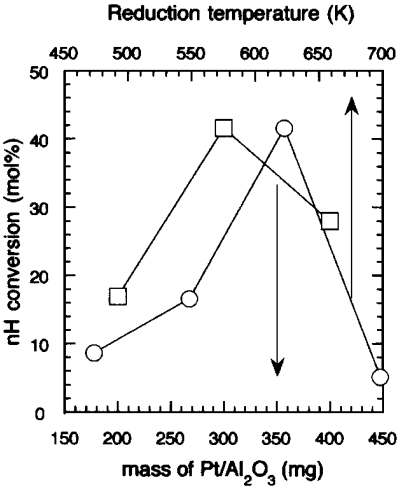

FIG. 1. Conversion of *n*-hexane at 423 K on a mechanical mixtures of SZ (100 mg of SZ(4)*isB*(3.2)) with Pt/Al_2O_3, as a function of the Pt/Al_2O_3 amount (reduction at 573 K), and the reduction temperature ($m(Pt/Al_2O_3) = 300$ mg).

3.2. Influence of the Water/Alkoxide Molar Ratio

The water/metal molar ratio in the sol–gel synthesis medium ($r = H_2O/Zr^{IV}$) was varied from 1 to 4 (stoichiometry at $r = 2$). The other parameters remained constant, and 0.51 cm^3 of sulfuric acid was added to the hydrolysis water.

Table 1 presents the conditions of sol–gel synthesis and the aspect of the "gel" as a function of *r*. A dense powder is obtained for $r = 1$ after solvent removal and further drying at 393 K, and for $r = 2$ after solvent removal at 348 K. Gels where always formed for $r > 2$ with a gelation time decreasing when *r* increases.

As reflected by TG-DSC and MS experiments (Figs. 2 and 3) water (mass 18) is similarly desorbed between 300 and 500 K, whatever the sample. In contrast, *r* influences the crystallization temperature into the tetragonal phase, which gives a first exotherm with a concurrent water evolution at 680 K for SZ(1)*isB*(3.4) and around 700 K for the other samples. A second broad exotherm appeared above 800 K, which is regularly shifted toward higher temperatures when *r* increases. This behavior, different from that of pure zirconia which shows only the sharp exotherm at a low temperature (22), results from the inhomogeneity in the crystal sizes of the sulfated samples (23). The crystallization is therefore delayed when *r* increases. This parameter also influences the stability of the sulfates and their decomposition process. The related endotherm above 800 K is shifted to higher temperatures as *r* goes on, while two main desorption peaks at 790 and 880 K (masses 48 and 64) are obtained

TABLE 1

Preparation Conditions and Characteristics of One-Step Sol–Gel Synthesized Sulfated Zirconia

Sample	H_2O/Zr^{IV}	Gelification	Crystallisation temperature (K)	S_{BET} at 898 K ($m^2\ g^{-1}$)	Mean pore diameter (nm)	S content (wt%) at 393 K	S content (wt%) at 898 K	S cont. at 898 K ($g_S\ m^{-2}$) × 10^5	nH reaction[a] Conv. (%)	nH reaction[a] TOF[b] (h^{-1})
SZ(1)*isB*(3.4)	1	No gel formation Light suspension	680–900	73	2.5	3.40	1.32	17.8	1.1	0.25
SZ(2)*isB*(2.4)	2	Light suspension Gel formation after heating at 323 K	700–900	45	2.9	2.40	2.27	49	3.6	0.47
SZ(3)*isB*(3.4)	3	Gel formation Stiring possible at high speed rate	700–923	74	3.0	3.40	2.0	27	12.1	1.8
SZ(4)*isB*(3.2)	4	Gel formation Stir bar blocked	700–973	88	3.0	3.20	1.80	20.4	42.5	7.1

[a] Standard conditions, samples calcined at 898 K.
[b] Turnover number, expressed per S atom.

for $r \leq 2$, but only one peak above 870 K for $r > 2$ (Fig. 3). For SZ(3)*isB*(3.4), 1-propene (mass 41), comes from either the dehydration of residual *n*-propanol or the decomposition of remaining *n*-propoxide ligands desorbed at 530 K, in relation with the exotherm at 520 K in the DSC profile.

These studies show that the temperature of crystallization is influenced by the water/metal ratio, but not by the sulfur content which is almost the same in all samples after calcination at 898 K (Table 1).

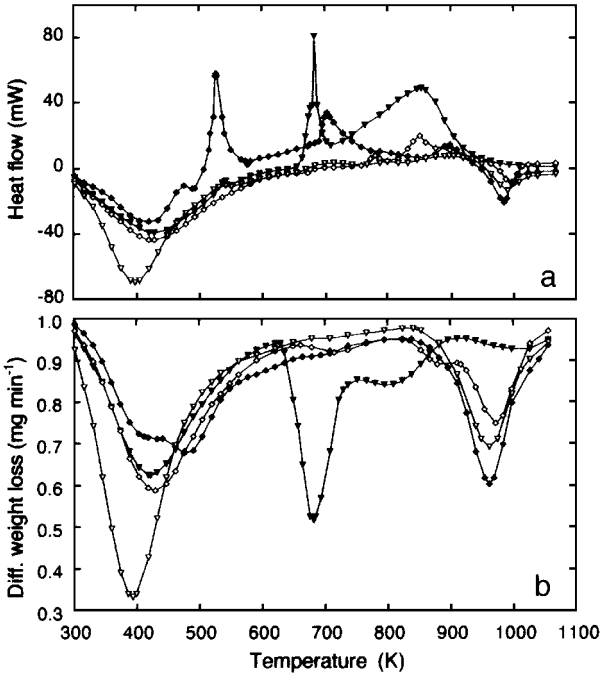

FIG. 2. The TG-DSC profiles for the SZ's when heated in a O_2/He (3/97) mixture: (a) heat flow, (b) differential weight loss; (▼) SZ(1)*isB*(3.4), (◇) SZ(2)*isB*(2.4), (◆) SZ(3)*isB*(3.4), (▽)SZ(4)*isB*(3.2).

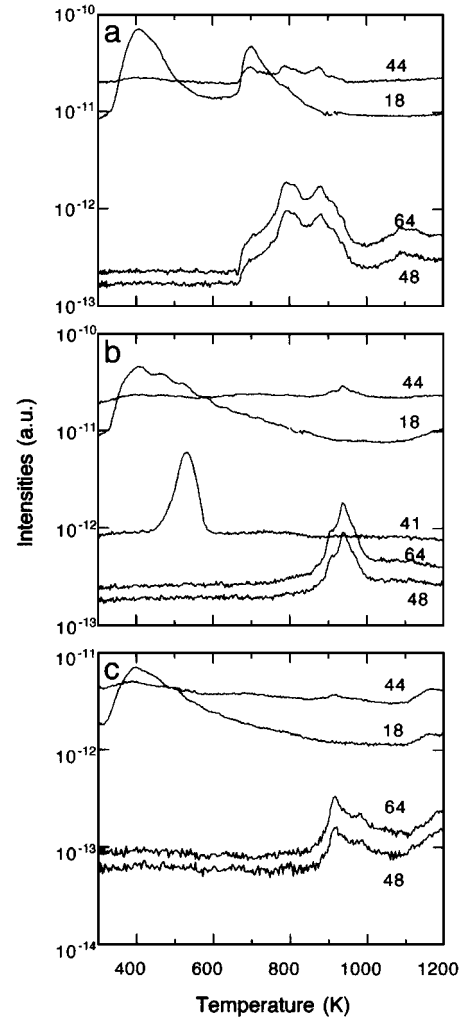

FIG. 3. MS profiles of the gases evolved during heating in a O_2/He (3/97) mixture of: (a) SZ(1)*isB*(3.4), (b) SZ(3)*isB*(3.4), (c) SZ(4)*isB*(3.2).

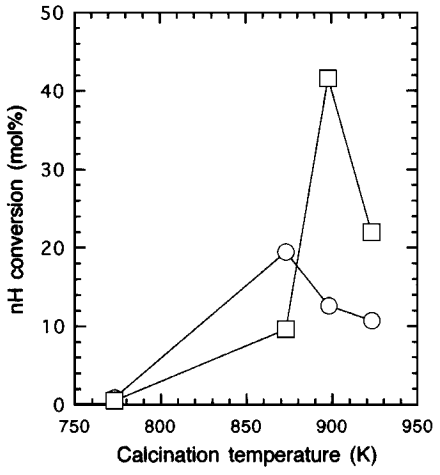

FIG. 4. Conversion of *n*-hexane at 423 K on a mechanical mixtures of SZ (100 mg) with Pt/Al_2O_3 (300 mg), as a function of the calcination temperature; (○) SZ(3)*isB*(3.4), (□) SZ(4)*isB*(3.2).

After calcination at 898 K, all samples exhibit a type-II isotherm of N_2 adsorption, according to the classification of Brunauer, without any hysteresis loop. The distribution of mesopores is narrow and between 1.5 and 4.0 nm. The SZ(2)*isB*(2.4) sample has the lowest specific surface area, differentiating it from the other samples. There is an increase of the volume in macropores of size larger than 30 nm when r increases. It comes from the intergranular space, which provides evidence of a decrease of the mean grain size.

The catalytic behavior of these materials were evaluated for the hydroconversion of nH over mechanical mixtures of SZ and Pt/Al_2O_3. The $r = 1$ sample was quasi-inactive under the present conditions, and the nH conversion went up for samples prepared with increasing r. Figure 4 presents nH conversion, after 10 min on-stream, as a function of the calcination temperature for two samples. Higher activities were reached after calcination at 873–903 K. It seems that the most active catalyst (SZ(4)*isB*(3.2)), which requires the highest temperature of calcination, also exhibits the narrower window of activity; a similar behavior was reported by Ward and Ko (5) for *n*-butane isomerisation over SZ's prepared by the sol–gel method, using a different procedure of preparation.

3.3. Influence of the Procedure for Sulfate Introduction

In a second step, SZ samples were prepared with $H_2O/Zr^{IV} = 4$ and according to different procedures for sulfate introduction: on the one hand, with H_2SO_4 in hydrolysis water (SZ(4)*isB*(3.2)) or in alkoxide solution (SZ(4)*isA*(3.2)); on the other hand, by *ex situ* sulfation of $Zr(OH)_4$ with H_2SO_4 (SZ(4)*esC*(5.9)). Preliminary results on these samples were reported previously (7). The samples were differentiated first with respect to the textural properties: SZ(4)*isA*(3.2) shows a broad pore size distribution between 3.0 and 20.0 nm centered around 10.0 nm, and SZ(4)*esC*(5.9), or SZ(4)*isB*(3.2), shows a narrower mesopore distribution between 1.5 and 3.5 nm in size. SZ(4)*isA*(3.2) exhibits textural properties close to that of zirconia obtained by precipitation of zirconyl chloride in an alkaline medium. By a one-step preparation similar to that used for the SZ(4)*isA*(3.2), sample, Ward and Ko (4) obtained a SZ which, after calcination at 773–873 K, exhibited a surface area of 110 $m^2\,g^{-1}$ and a pore size distribution from 4.5 to 8.0 nm. After calcination at 923 K, SZ(4)*esC*(5.9) was less active than SZ(4)*isA*(3.2) and SZ(4)*isB*(3.2) for the hydroconversion of nH (7).

However, by varying the calcination temperature we found that the samples, inactive below 800 K, exhibit the highest nH conversion for an optimum temperature of calcination which slightly differs from sample to sample. Table 2 reports some catalytic properties of the samples calcined at their optimum temperature.

These different responses of the samples to the temperature of calcination, could be related to the activation of

TABLE 2

Some Characteristics of Sulfated Zirconia Prepared According to Different Protocols for Sulfate Introduction and Calcined at Optimum Temperature

Sample	Optimum calcination temp.[a] (K)	S_{BET}[b] ($m^2\,g^{-1}$)	Mean pore diameter[b,c] (nm)	S content (wt%) after calcination at		S content[b] ($g_S\,m^{-2}$) × 10^5	nH reaction[b,d]	
				393 K	Optimum temp.[a] (K)		Conv. (mol%)	TOF[e] (h^{-1})
SZ(4)*esC*(5.9)	948	84	3.3	5.9	0.94	11.2	1.1	0.35
SZ(4)*isB*(3.2)	898	88	3.0	3.20	1.80	20.4	42.5	7.15
SZ(4)*isA*(3.2)	873	137	10.0	3.20	1.99	14.5	32.3	4.85

[a] Temperature of calcination for which nH conversion is maximum.
[b] After calcination at optimum temperature.
[c] From adsorption isotherm.
[d] Standard conditions.
[e] Turnover number, expressed per S atom.

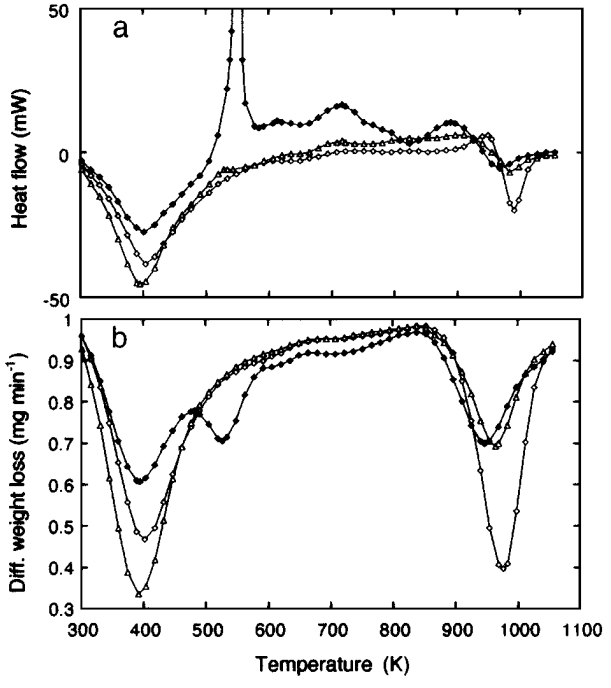

FIG. 5. The TG-DSC profiles for the SZ's when heated in a O_2/He (3/97) mixture; (a) heat flow, (b) differential weight loss; (◇) SZ(4)*esC*(5.9), (◆) SZ(4)*isA*(3.2), (△) SZ(4)*isB*(3.2).

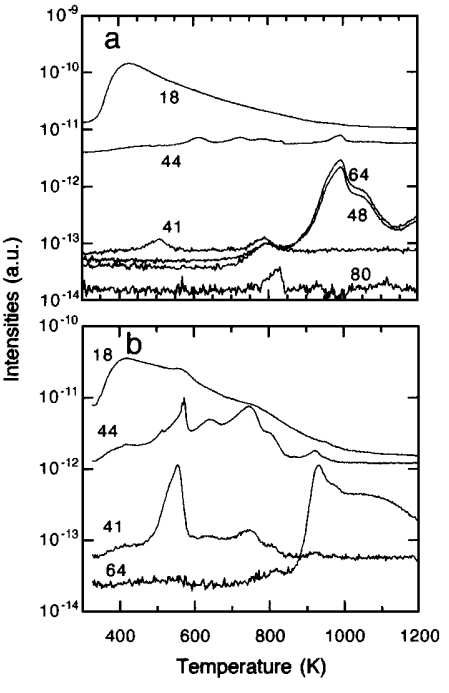

FIG. 6. MS profiles of the gases evolved during heating in O_2/He (3/97) mixture of: (a) SZ(4)*esC*(5.9), (b) SZ(4)*isA*(3.2).

sulfur species. The heating in an air stream of these solids from 300 to 1200 K was followed by TG-DSC and MS experiments (Figs. 5 and 6). Their behaviors during this activation treatment are similar, with (i) the endothermic H_2O desorption from 300 to 700–800 K and (ii) the decomposition and desorption of sulfur species which peaked at 920 K for SZ(4)*isB*(3.2), 930 K for SZ(4)*isA*(3.2), and 990 K for SZ(4)*esC*(5.9). In addition, for SZ(4)*isA*(3.2) a sharp desorption of 1-propene peaks at ca 550 K. The second exotherm of crystallization into the tetragonal phase above 800 K is superimposed on the endotherm of the sulfate decomposition. The comparison of SZ(4)*isB*(3.2) and SZ(4)*esC*(5.9) shows that these two phenomena are concurrently shifted to higher temperatures. This is in line with the stabilizing effect of sulfur (1). For SZ(4)*isB*(3.2) the ratio between masses 64 and 48 (≈0.5) is close to the fragmentation of SO_2 (Fig. 3c). In contrast, the intensity of mass 48 is much higher with SZ(4)*esC*(5.9) which provides evidence of a different decomposition process of the sulfate species (Fig. 6a). Albeit SO is extremely unstable, Srinivasan *et al.* (24) proposed its occurrence in relation to the peak of mass 48. In the absence of a clear identification of these evolved species, they will thereafter be denominated as SO_x.

3.4. Influence of Sulfate Content

Figures 7 and 8 present the results from TG-DSC and MS experiments for the activation of SZ prepared with increasing S content (Table 3). During these experiments the H_2O/Zr^{IV} molar ratio was maintained at 4 and H_2SO_4 was introduced via the hydrolysis water (method *isB*). It is worth noting that the exotherms, related to the crystallization

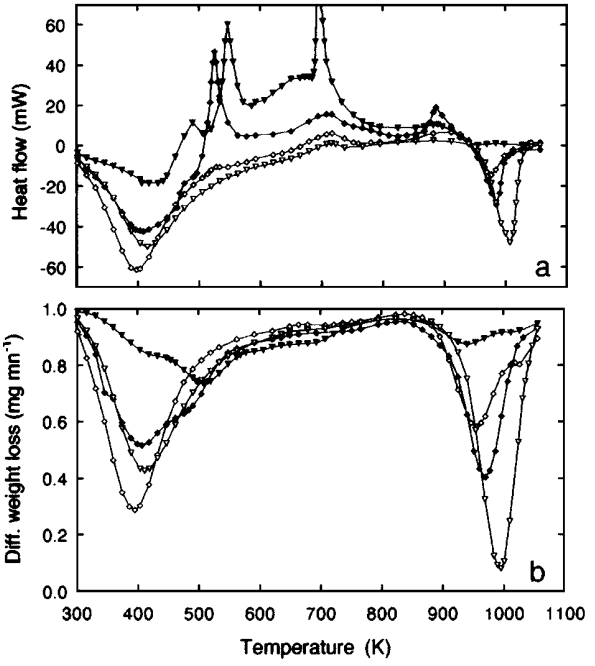

FIG. 7. The TG-DSC profiles for the SZ's when heated in a O_2/He (3/97) mixture; (a) heat flow, (b) differential weight loss; (▼) SZ(4)*isB*(2.1), (◇) SZ(4)*isB*(3.6), (◆) SZ(4)*isB*(4.9), (▽) SZ(4)*isB*(6.5).

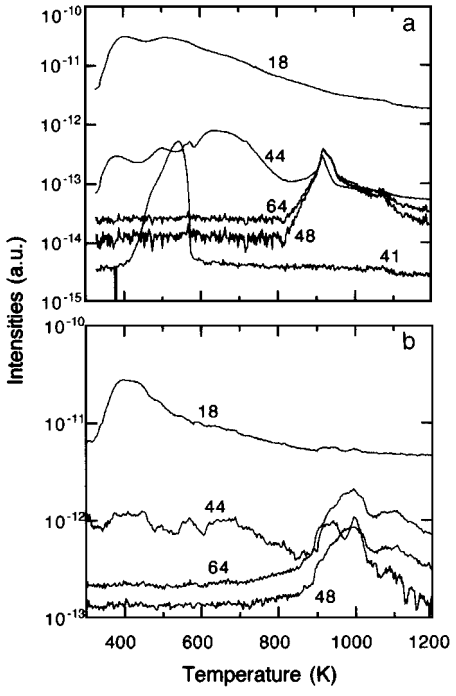

FIG. 8. MS profiles of the gases evolved during heating under O_2/He (3/97) mixture of: (a) SZ(4)*isB*(2.1), (b) SZ(4)*isB*(6.5).

into the tetragonal phase, are monotonously broadened with increasing the sulfur content. Dehydration and dehydroxylation occur during the crystallization, as shown by the H_2O release in the same temperature range. This is in agreement with the well-documented mechanism of zirconia formation from zirconium hydroxide, involving the loss of water and terminal hydroxo groups and then oxolation of OH bridges (22). Sulfate, which decomposed above 800 K, as shown by the related endotherm event, hinders the oxolation and the sintering of the crystals. Their growth is delayed and the tetragonal crystallites are still detected at 923 K. This is also the case for the monoclinic phase, since the transition from the tetragonal into the monoclinic phase occurs

TABLE 3

Some Characteristics of Sulfated Zirconia with Different Sulfur Contents

Sample	S_{BET}[a] ($m^2\ g^{-1}$)	S content (wt%) after calcination at 393 K	898 K	S content[a] ($g_S\ m^{-2}) \times 10^5$	nH reaction[a,b] Conv. (mol%)	TOF[c] (h^{-1})
SZ(4)*isB*(2.1)	66	2.10	1.01	15.3	11.5	3.45
SZ(4)*isB*(3.6)	89	3.60	1.75	19.8	25.7	4.40
SZ(4)*isB*(4.9)	101	4.90	2.10	20.7	41.7	6.00
SZ(4)*isB*(6.5)	55	6.50	5.35	97	13.3	0.75

[a] After calcination at 898 K.
[b] Standard conditions.
[c] Turnover number, expressed per S atom.

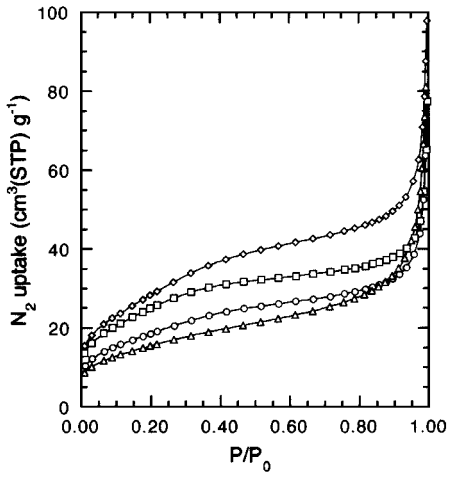

FIG. 9. N_2 adsorption isotherms at 77 K of SZ; (○) SZ(4)*isB*(2.1), (□) SZ(4)*isB*(3.6), (◇) SZ(4)*isB*(4.9), (△) SZ(4)*isB*(6.5).

when the size of the crystals becomes higher than a critical value (25).

There was a 1-propene evolution during the activation of the SZ(4)*isB*(2.1), sample at ca 520 K (Fig. 8a). This behavior parallels that previously observed for SZ(4)*isA*(3.2) and SZ(3)*isB*(3.4). The maxima of sulfate decomposition and SO_x evolution were shifted to higher temperatures (940 → 1000 K) as the S content increased in the uncalcined sample. At the lowest S content (SZ(4)*isB*(2.1)), the 64/48 peak intensity ratio is close to 1, which provides evidence of a concurrent evolution of SO_2 and SO_x (Fig. 8a). This is not the case at higher S content, where this ratio was close to 0.5, with SO_2 evolution mainly.

The textural properties of these samples, prepared with the same H_2O/Zr^{IV} ratio, are very similar, as shown in Fig. 9. Every sample shows a type-II isotherm and no hysteresis loop was identified on the desorption curve. The volume in mesopores reached a maximum value for SZ(4)*isB*(4.9).

Whatever the S content the faster rate of nH hydroconversion was reached after calcination at 898 K. The main characteristics and catalytic properties of the samples after calcination at 898 K are listed in Table 3. In the range of sulfate contents studied, the sulfur amount which gave the higher nH conversion is 2.10 wt% for SZ(4)*isB*(4.9) after calcination at 898 K. This value, which corresponds to $20.7\ 10^{-5}\ g_S\ m^{-2}$, is very close to the theoretical value giving a monolayer of sulfate. The monolayer coverage by sulfate species was claimed to give the higher reactive surface for alkane conversion (26).

4. DISCUSSION

The amount and the way by which sulfate was introduced in the hydrolysis medium have an influence on the textural, structural, and, therefore, the catalytic properties of

SZ prepared by sol–gel methods. The textural properties are dictated by the macroscopic conditions of the hydrolysis and condensation steps. More precisely, the H_2O/Zr^{IV} molar ratio influences the macroporosity of the final material, whereas the procedure followed for introducing H_2SO_4 seems to determine better the mesoporosity. Whatever the sulfur content and the H_2O/Zr^{IV} ratio, when H_2SO_4 is introduced via the hydrolysis water, the samples calcined at 898 K exhibit type-II nitrogen adsorption isotherms, with mesopores centered around 3.0 nm. On the other hand, when the H_2O/Zr^{IV} ratio increases the volume in macropores increases, too, very likely in the intergrain domain. During the activation of SZ(3)*isB*(3.4), SZ(4)*isA*(3.2), and SZ(4)*isB*(2.1) samples under air (Figs. 3b, 6b, and 7a), there was an evolution of 1-propene. The occurrence of this phenomenon with SZ(4)*isB*(2.1) and SZ(3)*isB*(3.4) samples discards any clear relationship between the singular textural properties of SZ(4)*isA*(3.2) and this 1-propene evolution. As suggested previously (7), the textural properties of SZ(4)*isA*(3.2) may be related to the prehydrolysis step included in the synthesis as previously reported for pure zirconia aerogels (27) or zirconia–silica aerogels (28). This prehydrolysis step could be induced by the trace amounts of water present in concentrated H_2SO_4. Indeed, the *in situ* sulfation appears different between the two one-step sol–gel procedures. Actually, when H_2SO_4 is previously mixed with $Zr(OC_3H_7)_4$ in *n*-propanol solution, there is a sharp gradient in the sulfate concentration at the interface between the microdomains of the alkoxide solution and the first drops of added water. This could modify the surface properties of the final SZ.

The evolution of 1-propene originates either from the solvent *n*-propanol, or from the *n*-propoxide ligand of zirconium. The 1-propene evolution peaked at 500–550 K for the different samples, and this value is independent of the texture and composition of the final catalyst. One could think that this 1-propene evolution would be better explained by a chemical process rather than by a flash desorption of *n*-propanol "trapped" in the bulk. This chemical process would likely be an alcohol condensation between $\equiv Zr{-}(nPrO)$ and $\equiv Zr{-}OH$ which leads to $\equiv Zr{-}O{-}Zr\equiv$ and *n*-propanol. *n*-Propanol thus formed will be promptly dehydrated on weakly acidic sites to 1-propene which desorbs. The result of this process is a reorganization, or a healing, of the network of the amorphous phase of zirconia, with the appearance of an exothermic event.

Besides the effect on the textural properties of SZ, the amount of sulfate, and the way in which it is introduced, influence also the catalytic properties. Tables 1–3 report the various samples' sulfur content per square meter and the activity for nH conversion, recorded after 10 min on-stream, expressed as the number of nH molecules transformed per nominal "sulfate site" and per hour, equivalent to a turnover frequency (TOF). The different behaviors of the samples might be related to the activation of the sulfate. It appears from the TG-DSC and MS experiments that the activation of sulfur species is rather complicated. Depending on the sample, between one to three SO_x evolutions occurred, at temperatures lower than 900 K (SZ(1)*isA*(3.4)), between 900 and 1000 K for every sample, and above 1000 K for some samples. Let us estimate roughly from the MS spectra the desorption temperature of the fraction of sulfate species retained by the samples after calcination at the temperature giving the higher reactivity. It thus appears that for SZ(4)*esC*(5.9), a poorly active sample, the last 15% of SO_x desorbs around 1050 K (Fig. 6a). This SO_x evolution should correspond to the ca 1 wt% S species retained after calcination at 948 K (Table 2). In contrast, the last 50–60% of SO_x evolution from SZ(4)*isB*(3.2) (Fig. 3c) and SZ(4)*isA*(3.2) (Fig. 6b) occurs between 950 and 1100 K, and these catalysts are very reactive. Eighty percent of SO_x evolves above 950 K from SZ(4)*isB*(6.5) (Fig. 8b), but this sample exhibits a poor activity. In contrast, 60% of SO_x evolves around 960 K from SZ(3)*isB*(3.4) (Fig. 3b), which shows a significant reactivity. No clear relationship thus appears between the catalytic activity and the high temperature SO_x evolution (>900 K). Actually, it seems that the temperature of the maximum SO_x desorption rate is mainly determined by the amount of sulfate species. This temperature is steadily shifted to higher values when the S content is increased, e.g. for SZ(4)*isB*(2.1), SZ(4)*isB*(3.6), SZ(4)*isB*(4.9), and SZ(4)*isB*(6.5) prepared according to the same procedure.

The most active catalysts turn out to be those prepared by the one-step sol–gel method, with $H_2O/Zr^{IV} = 4$, and a sulfur content corresponding to a monolayer of sulfate after calcination at 870–900 K. In agreement with Ward and Ko (5), the activation of sulfate species in these samples can be understood according to the following sequence. First, after drying at 393 K, the sulfate groups replace hydroxyl groups to form bidentate chelating or bridging sulfate groups. Second, after calcination at 800 K, in the course of the transition from amorphous to tetragonal phases, these species migrate to the surface and create potentially active sites. Third, these surface species start to decompose and evolve as SO_x around 850 K. Finally, optimal activation is reached after calcination at about 900 K with formation of a theoretical "monolayer" coverage of zirconia by sulfate ($\approx 21 \times 10^{-5}$ g_S m^{-2}). However, the comparison of SZ(4)*isB*(2.1) (15.3×10^{-5} g_S m^{-2}) and SZ(4)*isA*(3.2) (14.5×10^{-5} g_S m^{-2}) illustrates that the S content is not the only factor governing activity. The conditions of crystallization of zirconia are also important. It was previously suggested that a higher acid strength in SZ is associated with Zr sites of low coordination, i.e. for high specific surface areas (29). In this context, the comparative behavior of SZ(4)*isB*(2.1) and SZ(4)*isA*(3.2) illustrates this proposal, since these samples exhibit 66 and 137 m^2 g^{-1}, respectively,

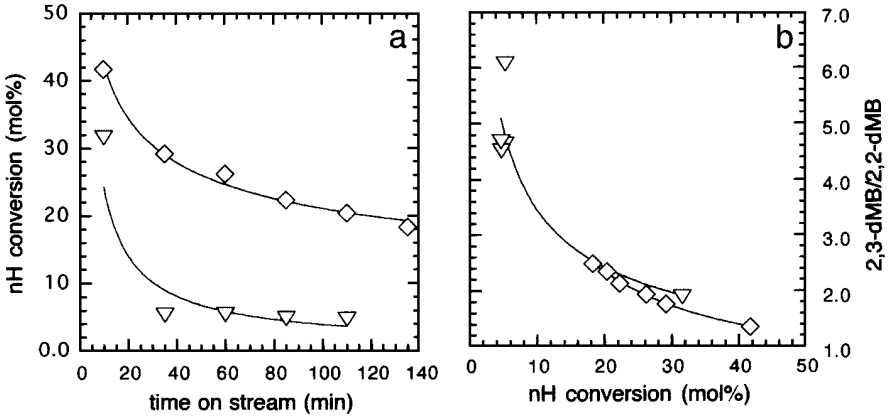

FIG. 10. (a) Conversion of *n*-hexane at 423 K as a function of time on stream on mechanical mixtures of SZ (100 mg) with Pt/Al_2O_3 (300 mg); (b) 2,3-dMB/2,2-dMB ratio as a function of nH conversion; (◇) SZ(4)*isB*(4.9), (▽) SZ(4)*isA*(3.2).

and a turnover of 3.45 and 4.85 h^{-1} respectively, in nH hydroconversion.

Figure 10a shows the conversion of nH over SZ(4)*isA*(3.2) and SZ(4)*isB*(4.9) catalysts as a function of time on-stream. It appears that SZ(4)*isB*(4.9) deactivates to a lesser extent than SZ(4)*isA*(3.2). The activity extrapolated to time zero on the latter sample might be higher than on the former. The faster deactivation rate of SZ(4)*isA*(3.2) could be the reflection of sites with higher acid strength on this sample. This conclusion is further substantiated by the high selectivity to cracked products, 44.5 mol% at 31% conversion, obtained with SZ(4)*isA*(3.2), compared to 3 mol% at 41% conversion for the SZ(4)*isB*(4.9) sample. However, the similarity between the values of the 2,3-dimethylbutane/2,2-dimethylbutane (2,3dMB/2,2dMB) ratio for SZ(4)*isA*(3.2) and SZ(4)*isB*(4.9) at the same conversion (≈30%, Fig. 10b) does not provide evidence for a large difference in acidity between these samples, since 2,2-dMB formation should be favoured when the acid strength increases. On the other hand, whatever the conversion, the molar composition of the 2,3-dMB, 2-methylpentane, and 3-methylpentane isomers is very close to thermodynamic equilibrium, and 2,2-dMB appears as a secondary product since the 2,3dMB/2,2dMB ratio increases when the conversion decreases (Fig. 10b). Anyway, even if some differences exist between the SZ samples prepared by the one-step sol–gel method, the main differences appear with this group of samples and that prepared, in the two-step method by *ex situ* sulfation (SZ(4)*esC*(5.9)). The latter is twentyfold less active, and, under the same reaction conditions, behaves very similarly as SZ prepared by the classical procedure from inorganic precursors (7). When comparing SZ(4)*isA*(3.2), SZ(4)*isB*(3.2), and SZ(4)*esC*(5.9) samples, there is no correlation between the catalytic activity and (i) the desorption temperature of sulfate species, (ii) the intensity of the IR S=O bands at 1400–1380 cm^{-1} (30), or (iii) the intensity of the OH band at 3640 cm^{-1} (31). It was indeed proposed that the intensity of the OH bands at 3740 cm^{-1} could be correlated with the high catalytic activity in *n*-butane isomerization on SZ prepared by a one-step sol–gel method (5); this band was not found in our spectra (31). In contrast, the IR spectra of SZ(4)*isA*(3.2), SZ(4)*isB*(3.2), and SZ(4)*esC*(5.9) samples show great differences in the 3400–2900 cm^{-1} range (31). In agreement with Kustov *et al.* (32), this broad band, shown by the SZ(4)*isA*(3.2) and SZ(4)*isB*(3.2) samples and composed of two individual contributions centered at ca 3260 and 3150 cm^{-1}, was attributed to acidic protons resulting from the substitution of the terminal −OH of ≡Zr−OH by HSO_4^- anions. The species responsible for this broad absorption band would be:

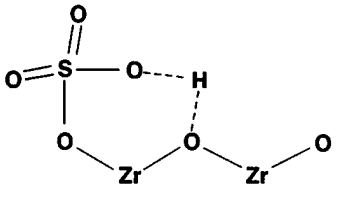

A DRIFT study of the adsorption of benzene on these SZ samples has been carried out (31). It was thus shown that hydroxyls associated with the band at 3640 cm^{-1} give simple hydrogen bonding and shift by about 200 cm^{-1} to lower frequencies upon benzene adsorption. The hydroxyls associated with the broad band at 3300–3100 cm^{-1} are able to exchange H with C_6D_6, which would involve protonation of benzene at room temperature.

5. CONCLUSION

We have shown that SZ's prepared by one-step *in situ* sol–gel methods, with H_2SO_4 in H_2O or in alkoxide solution, are up to twentyfold more active in nH hydroconversion at 423 K than SZ's prepared by *ex situ* sulfation.

The key preparation parameters governing the SZ reactivity are a H_2O/Zr^{IV} hydrolysis ratio $r \geq 3$, and a S content close to a nominal monolayer coverage by sulfate species ($\approx 21 \times 10^{-5}$ g_S m^{-2}), after calcination around 900 K. The way by which sulfate anions are introduced, either through hydrolysis water or through Zr *n*-propoxide solution, is of secondary importance. However, the way in which sulfate is introduced affects the textural properties. A narrow distribution of small mesopores centered around 2–3 nm can be obtained with H_2SO_4 in H_2O, whereas sulfate introduced in Zr *n*-propoxide solution leads to solids with a wide distribution of large mesopores from 3 to 20 nm.

It seems that the superior reactivity of one-step *in situ* SZ's is correlated with the acidic OH groups which give a broad and intense IR absorption band around 3250 cm^{-1} (31). This band will be due to the substitution of terminal ZrOH groups by HSO_4^- anions (32). This IR band was absent from the SZ prepared by *ex situ* sulfation.

ACKNOWLEDGMENT

H.A. warmly thanks the CONACYT of Mexico for a grant.

REFERENCES

1. Arata, K., *Adv. Catal.* **37**, 165 (1990).
2. Hino, M., Kobayashi, S., and Arata, K., *J. Am. Chem. Soc.* **101**, 6439 (1979).
3. Ebitani, K., Konishi, J., and Hattori, H., *J. Catal.* **130**, 257 (1991).
4. Ward, D. A., and Ko, E. I., *J. Catal.* **150**, 18 (1994).
5. Ward, D. A., and Ko, E. I., *J. Catal.* **157**, 321 (1995).
6. (a) Signoretto, M., Pinna, F., Strukul, G., Cerrato, G., and Morterra, C., *Catal. Lett.* **36**, 129 (1996). [(b) Morterra, G., Cerrato, G., Di Ciero, S., Signoretto, M., Pinna, F., and Strukul, G., *J. Catal.* **165**, 172 (1997)]
7. Tichit, D., Coq, B., Armendariz, H., and Figuéras, F., *Catal. Lett.* **38**, 109 (1996).
8. Brinker, C. J., and Scherer, G. W., *in* "Sol–Gel Science," Academic Press, San Diego, 1990.
9. Ebitani, K., Konno, H., Tanaka, T., and Hattori, H., *J. Catal.* **135**, 60 (1992).
10. Garin, F., Andriamasinoro, D., Abdulsamad, A., and Sommer, J., *J. Catal.* **131**, 199 (1991).
11. Davis, B. H., Keogh, R. A., and Srinivasan, R., *Catal. Today* **20**, 219 (1994).
12. Iglesia, E., Soled, S. L., and Kramer, G. M., *J. Catal.* **144**, 238 (1993).
13. Yori, J. C., D'Amato, M. A., Costa, G., and Parera, J. M., *J. Catal.* **153**, 218 (1995).
14. Yori, J. C., and Parera, J. M., *Appl. Catal. A: General* **129**, 83 (1995).
15. Comelli, R. A., Finelli, Z. R., Vaudagna, S. R., and Figoli, N. S., *Catal. Lett.* **45**, 227 (1997).
16. Sayari, A., and Dicko, A., *J. Catal.* **145**, 561 (1994).
17. Paal, Z., Mulher, M., and Schlögl, R., *J. Catal.* **143**, 318 (1994).
18. Zhao, J., Huffman, G. P., and Davis, B. H., *Catal. Lett.* **24**, 385 (1994).
19. Coq, B., Walter, C., Brown, R., McDougall, G., and Figuéras, F., *Catal. Lett.* **39**, 197 (1996).
20. Weisz, P. B., *Adv. Catal.* **13**, 137 (1962).
21. Xu, B.-Q., and Sachtler, W. M. H., *J. Catal.* **167**, 224 (1997).
22. Mercera, P. D. L., Van Ommen, J. G., Doesburg, E. B. M., Burggraaf, A. J., and Ross, J. R. H., *Appl. Catal.* **57**, 127 (1990).
23. Norman, C. J., Goulding, P. A., and McAlpine, I., *Catal. Today* **20**, 313 (1994).
24. Srinivasan, R., Keogh, R. A., Milburn, D. R., and Davis, B. H., *J. Catal.* **153**, 123 (1995).
25. Garvie, C. G., *J. Phys. Chem.* **69**, 1238 (1965).
26. Nascimento, P., Akratopoulos, C., Oszagyan, M., Coudurier, G., Travers, C., Joly, J. F., and Védrine, J., *in* "Proceeding 10th International Congress on Catalysis" (L. Guczi, F. Solymosi, and P. Tétényi, Eds.), Vol. B, p. 1185, Akad. Kiado, Budapest, 1993.
27. Ward, D. A., and Ko, E. I., *Chem. Mat.* **5**, 956 (1993).
28. Miller, J. B., Rankin, S. E., and Ko, E. I., *J. Catal.* **148**, 673 (1994).
29. Tichit, D., El Alami, D., and Figuéras, F., *J. Catal.* **163**, 18 (1996).
30. Armendariz, H., Ph.D. thesis, Montpellier, January 1997.
31. Armendariz, H., Sanchez Sierra, C., Figuéras, F., Coq, B., Mirodatos, C., Lefebvre, F., and Tichit, D., *J. Catal.* **171**, 85 (1997).
32. Kustov, L. M., Kazansky, V. B., Figuéras, F., and Tichit, D., *J. Catal.* **150**, 143 (1994).